ELSEVIER

Physica D 81 (1995) 94–110

PHYSICA D

Quenching and propagation of bistable reaction-diffusion fronts in multidimensional periodic media

Jack X. Xin [a], Jingyi Zhu [b]

[a] Department of Mathematics, University of Arizona, Tucson, AZ 85721, USA

[b] Department of Mathematics, University of Utah, Salt Lake City, UT 84112, USA

Received 8 September 1993; revised 5 October 1994

Communicated by C.K.R.T. Jones

Abstract

We study the front dynamics of the bistable reaction-diffusion equations with periodic diffusion and/or convection coefficients in several space dimensions. When traveling wave solutions exist, the solutions of the initial value problem behave as wave fronts propagating with the effective speeds of traveling waves under various initial conditions. Yet due to the bistable nature of the nonlinearity, traveling waves may not always exist when the medium variations from the mean states are large enough. Their existence is closely related to the detailed forms of diffusion and convection coefficients, more so in multidimension than in one. We present a simple sufficient condition for the nonexistence of traveling waves (quenching) using perturbation method. Our two dimensional finite difference numerical computations show a variety of front behaviors, such as: the propagation, quenching and retreat of fronts. We found numerically that quenching occurs in two space dimensions when diffusion is spatially uniform and convection field is a periodic array of rotating vortices if the root mean square of the convection field reaches a critical number.

1. Introduction

In this paper, we study the front dynamics of the solutions of the following reaction-diffusion (R-D) equations:

$$\begin{aligned} u_t &= \nabla_x \cdot (a(x)\nabla_x u) + b(x)\cdot\nabla_x u + f(u), \\ u|_{t=0} &= u_0(x), \end{aligned} \tag{1.1}$$

under the assumptions:

(A1) $a(x) = (a_{ij}(x))$, $x = (x_1, x_2, \cdots, x_n) \in \mathbb{R}^n$ is a smooth positive-definite matrix on $\mathbb{R}^n$, 1-periodic in each direction x_i;

(A2) $b(x) = (b_j(x))$ is a smooth divergence free vector field, 1-periodic in each direction x_i, and has mean equal to zero;

(A3) $f(u)$ is a bistable nonlinearity, i.e., $f(u) = u(1-u)(u-\mu)$, for some $\mu \in (0, 1/2)$.

SSDI 0167-2789(94)00204-5

The simple form of the function f in (A3) is chosen for convenience, and more general bistable nonlinearities will not essentially change the results in this paper. The initial condition $u_0(x)$ is continuous and ranges between 0 and 1.

Equations of the form (1.1) appear in the study of premixed flame propagation through turbulence media, see Clavin and Williams [13], where u is the temperature of the combustible gas, $b(x)$ is the prescribed turbulent incompressible fluid velocity field with zero ensemble mean, $f(u)$ is the Arrhenius reaction term, and $a(x)$ is taken as a constant matrix. In [13], based on their formal asymptotic analysis in the large activation temperature limit, Clavin and Williams found that the temperature "profile" u propagates with effective turbulent flame speed. To avoid the difficulty of dealing with complex flows involving a wide range of spatial and temporal scales such as turbulence, we consider here the very special periodic case. Typically, the flow fields $b(x)$ are made of a periodic array of vortices. As we will see, this simplification preserves the basic propagation feature of the problem and the related dynamic properties of solutions; moreover it eases our task of understanding the interaction between nonlinearities and inhomogeneities. For a work in the same spirit, see Berestycki and Sivashinsky [10].

The inhomogeneous diffusion matrix $a(x)$ arises in solute transport problems of hydrology, see Dagan and Neuman [15], where u is the concentration of the solute substance, $b(x)$ is the steady incompressible fluid velocity with homogeneous statistics, and $a(x)$ is the so called pore-scale dispersion tensor. Eq. (1.1) is thus related to both of these applications above on a formal level.

When $f(u)$ is a combustion nonlinearity, which is an approximation of the Arrhenius reaction with an ignition temperature cutoff (see Berestycki, Nicolaenko and Scheurer [4], Berestycki and Larrouturou [8] among others), traveling wave solutions exist for any $a(x)$ and $b(x)$ satisfying (A1),(A2), see Xin [34]. They are of the form $u = U(k\cdot x - ct, x)$, where k is a constant unit vector in $\mathbb{R}^n$, $c = c(k)$ is the unknown wave speed along direction k; U as function of $s \equiv k\cdot x - c(k)t$, and $y \equiv x$, satisfies the boundary conditions $U(-\infty, y) = 0$, $U(+\infty, y) = 1$, and $U(s,\cdot)$ has period 1. Moreover, for a large class of front-like or pulse-like initial conditions, the solutions of the initial value problem behave as wave fronts propagating with the effective speeds $c(k)$ of the traveling waves in all suitable directions, see Xin [35]. This is then the mathematical justification in the periodic case of the effective propagation phenomena of flame fronts in statistically homogeneous media as observed by Clavin and Williams.

When $f(u)$ is the KPP (the Kolmogorov–Petrovsky–Piskunov) nonlinearity, e.g. $f(u) = u(1-u)$, effective wave front propagation is shown in periodic case as well as in one-space-dimensional random case for pulse-like initial data, see Freidlin [18]. He uses probabilistic representation and large deviation techniques, which seem to work only for the KPP-like nonlinearities.

One common feature of the combustion and KPP nonlinearities is that they do not change sign on the interval $[0,1]$. The fact that the bistable nonlinearities change sign on $[0,1]$ makes it much harder to obtain a general existence theory of traveling waves for (1.1). In fact, there are examples (both analytical and numerical) in the one space dimension showing that standing waves taking 0 and 1 at infinities exist when the variations of the media are large enough, see Xin [35]. By maximum principle, this implies that traveling waves do not exist in those examples and quenching occurs. Quenching does not occur for Eq. (1.1) if $f(u)$ is a combustion or KPP nonlinearity, see Xin [34] and Freidlin [18]. On the other hand, we know that traveling waves exist up to a critical level of medium variation, see Xin [32] and [34]. Whether one can remove the critical obstruction to existence is a case by case issue.

In this paper, we derive a sufficient condition for nonexistence or quenching of multidimensional traveling waves by perturbing around the known stationary solution of the constant coefficient bistable reaction-diffusion equation with $\mu = 1/2$. The sufficient (quenching) condition comes as the solvability condition of the perturbation scheme for constructing a stationary solution to Eq. (1.1). We show both positive examples that satisfy the quenching conditions and negative ones where the quenching condition fails and we are unable to conclude analytically. In our numerical simulation of the positive examples, quenching indeed occurs. We also observe the subsequent retreat of fronts and offer our interpretations of this phenomenon. One of the most interesting negative examples is when $a(x)$ is the identity matrix, and $b(x)$ satisfies (A2). Existence of traveling waves or standing waves holds if $b(x)$ is a shear flow and waves are moving along the shearing direction. This follows easily from the work of Berestycki and Nirenberg [7]. It seems not obvious when the standing waves appear, and we have not observed them within the scope of our numerical computations. How about other kind of divergence free mean zero flows? Our numerical computations indicate that quenching occurs in two space dimensions when $b(x)$ is a periodic array of rotating vortices if the root mean square value of the flow fields reaches certain critical number.

The rest of the paper is organized as follows. In Section 2, we review the known existence theory of traveling waves as well as the propagation theorems if the traveling waves exist. In Section 3, we present the sufficient quenching condition, and examples that satisfy or fail to satisfy this condition. In Section 4, we describe the details of our finite difference schemes, and the constructions of the rotating vortex flow field. In Section 5, we show the numerical results for the examples in Section 3 when the space dimension is equal to two. Section 6 is the final conclusion.

2. Traveling waves and front propagation

We consider the traveling waves solutions of Eq. (1.1) of the form $u(x,t) = U(k\cdot x - ct, x)$, where k is a constant vector in $\mathbb{R}^n$; c, the wave speed, is an unknown constant depending on k; U, as a function of $s = k\cdot x - ct$, and $y = x$, satisfies the boundary conditions $U(-\infty, y) = 0$, $U(+\infty, y) = 1$, and $U(s,\cdot)$ has period 1. Upon substitution into Eq. (1.1), we obtain the following equation for $U = U(s,y)$ and c:

$$\begin{aligned}&(k\partial_s + \nabla_y)(a(y)(k\partial_s + \nabla_y)U) + b(y)\cdot(k\partial_s + \nabla_y)U + cU_s + f(U) = 0,\\ &U(-\infty, y) = 0, \quad U(+\infty, y) = 1, \quad U(s,\cdot) \text{ has period } 1\end{aligned} \tag{2.1}$$

Eq. (2.1) is a degenerate elliptic equation on the infinite cylinder $\mathbb{R}^1 \times T^n$, T^n being the n-dimensional unit torus. We have

Theorem 2.1. (Existence). Let $\bar{a} = \int_{T^n} a(x)dx$, and assume that (A1)–(A3) are valid. There is a positive number δ_{cr}, such that if $\|a(x) - \bar{a}\|_{H^s(T^n)} < \delta_{cr}$, and $\|b(x)\|_{H^s(T^n)} < \delta_{cr}$, where $s = s(n) > n+1$, there exist classical solutions $(U(s,y),c)$ of Eq. (2.1) satisfying all the boundary conditions, and that

$$0 < U < 1, \quad \forall (s,y) \in \mathbb{R}^1 \times T^n, \tag{2.2}$$

$$U_s > 0, \quad \forall (s,y) \in \mathbb{R}^1 \times T^n, \tag{2.3}$$

$$c < 0. \tag{2.4}$$

For a proof, we refer to Xin [35] or [32] and [34]. The number δ_{cr} may be infinite. The following are main properties of traveling waves if they exist.

Theorem 2.2. (Monotonicity and Uniqueness). Under assumptions (A1)–(A3), any classical solutions (U,c) satisfy (2.2), (2.3), and (2.4). Moreover, if (U',c') is another classical solution, then $c' = c$, and $U'(s,y) = U(s+s_0, y)$ for some $s_0 \in \mathbb{R}^1$.

We refer to Xin [33] for a proof.

Remark 2.1. For corresponding theorems when $f(u)$ is a combustion nonlinearity, see Xin [35]. In particular, existence of traveling waves holds without restriction on the variation of coefficients from their mean states as may happen in Theorem 2.1.

Assuming that the traveling waves exist, we have

Theorem 2.3. (Front Propagation). Let us consider the initial value problem for Eq. (1.1) with initial data $0 \le u_0(x) \le 1$. Assume that the traveling wave solutions $U(k\cdot x - c(k)t, x)$ exist, for any unit vectors $k \in \mathbb{R}^n$. Let $s \in \mathbb{R}^1$ and define the plane orthogonal to k by $S = S(k)$, i.e.

$$S = \{y \in \mathbb{R}^n | y = x - (k\cdot x)k, \quad \forall x \in \mathbb{R}^n\}.$$

I. Suppose that

$$\limsup_{k_0\cdot x \to -\infty} u_0(x) < \mu,$$
$$\liminf_{k_0\cdot x \to +\infty} u_0(x) > \mu,$$

uniformly in $S(k_0)$, for some $k_0 \in \mathbb{R}^n$. Then

$$\lim_{t\to\infty} u(t, sk_0t) = \begin{cases} 1, \ if & s > c(k_0), \\ 0, \ if & s < c(k_0). \end{cases}$$

II. Suppose that

$$\limsup_{|x|\to +\infty} u_0(x) < \mu,$$
$$u_0(x) > \mu + \eta, \qquad \text{for } |x| < L,$$

where η and L are positive constants, and $L \ge L_0 = L_0(\eta) > 0$. Then

$$\lim_{t\to\infty} u(t, skt) = \begin{cases} 1, & \text{if } c(k) < s < -c(-k), \\ 0, & \text{if } s < c(k) \text{ or } s > -c(-k). \end{cases}$$

For a proof, we refer to Xin [35].

Suppose now that $a(x)$ is the identity matrix, $b(x) = (b_j(x))$, $j = 1, \cdots, n$, $b_1(x) = b_1(x_2, \cdots, x_n)$, and $b_j(x) = 0$, for $j \ge 2$. This kind of vector fields $b(x)$ is often called shear flows. Let us consider traveling waves going along x_1 direction, i.e., $k = (1, 0, \cdots, 0)$, $U = U(x_1 - ct, y)$, where $y = (x_2, \cdots, x_n)$. Note that the traveling waves along x_j, $j \ge 2$, directions are just the waves in the constant coefficient problem. Eq. (2.1) now reduces to

$$\triangle_{s,y} U + (c + b_1(y))U_s + f(U) = 0,$$
$$U(-\infty, y) = 0, \quad U(+\infty, y) = 1, \quad U(s, \cdot) \text{ has period } 1. \tag{2.5}$$

We have

Theorem 2.4. (Existence, Shear Flows). Consider Eq. (2.5) with a smooth mean zero periodic function $b_1(y)$ and its boundary conditions. Then there exist unique solutions $(U(s,y), c)$ up to constant translation in s, and (U, c) satisfy (2.2) and (2.3).

We remark that Eq. (2.5) describes both traveling waves (if $c \neq 0$) and standing waves (if $c = 0$), while Eq. (2.1) in general only makes sense for traveling waves ($c \neq 0$). In other words, traveling waves and standing waves are of different functional forms except in the special shear flow case. It seems not obvious that the wave speed c in (2.5) is never zero. However, within the range of our numerical calculations, we have not observed any standing waves. For details of the numerical schemes we use, see Section 4.

The proof of the above theorem follows that of Theorem 1.3 in Berestycki and Nirenberg [7] where they showed the existence of a solution to Eq. (2.5) with y belonging to a bounded convex domain ω of R^{n-1}, and U_ν, the exterior normal derivative of U on the boundary of cylindrical domain $\omega \times \mathbb{R}^1$, equal to zero. Their proof relies on the fact that any nonconstant solution of the problem

$$\triangle_y u + f(u) = 0, \quad y \in \omega, \tag{2.6}$$

$$u_\nu = 0, \quad y \in \partial\omega, \tag{2.7}$$

is unstable if ω is convex. Problem (2.6) is the limiting equation of (2.5) as s tends to infinities, since U_s vanishes in the limit. The instability of a solution u means that the linearized operator around it:

$$\triangle_y \psi + f'(u)\psi, \tag{2.8}$$

has a positive principal eigenvalue with the same Neumann boundary condition.

The instability of nonconstant solutions is even easier to see in case of periodic boundary condition. Actually, differentiating Eq. (2.6) with respect to y_j, $j = 1, \ldots, n$, shows that each of $\partial_{y_j} U$ is in the kernel of the linearized operator (2.8). If U is nonconstant, then one of them should be nonzero, hence an eigenfunction corresponding to the eigenvalue zero. Obviously, $\partial_{y_j} U$ cannot have a definite sign, since its average over T^{n-1} is zero. By the Krein–Rutman theorem, the principal eigenvalue should be the largest one on the real axis and the principal eigenfuntion should be strictly positive (negative). Thus zero is not the principal eigenvalue, and the principal eigenvalue must be positive. We refer to [7] for all the other details of the proof.

3. A sufficient condition for quenching

In this section, we derive a sufficient condition for quenching in any space dimensions. For convenience, we construct stationary solutions to Eq. (1.1) along the x_1 direction.
Set $x = (x_1, y)$, $y = (x_2, \cdots, x_n)$ and consider the problem:

$$\nabla_x(a(x)\nabla_x u) + b(x) \cdot \nabla_x u + \mu^2 f(u) = 0, \tag{3.1}$$

$$u(-\infty, y) = 0, \quad u(+\infty, y) = 0, \quad \langle u(0,y)\rangle_y = 1/2, u(x,\cdot) \text{ has period } 1 \tag{3.2}$$

where $a(x) = Id + \delta\lambda a_1(x)$, $|\delta| \ll 1$, $\lambda \in \mathbb{R}^1$, $a_1(x) = (a_1^{ij}(x))$ is a smooth 1-periodic symmetric n by n matrix; $b(x) = \delta\lambda b_1(x)$, where $b_1(x) = (b_{1,j}(x))$ is a smooth mean zero divergence free vector field; μ is a positive constant, $f(u) = u(1-u)(u - \frac{1}{2} + \delta)$; $\langle\cdot\rangle_y$ means taking the average of the function inside the bracket over $y \in T^{n-1}$.

Write $u = \varphi^\mu(x_1) + \delta v(x)$, and $f(u) = f_0(u) + \delta u(1-u)$, where $f_0(u) = u(1-u)(u - \frac{1}{2})$, and $\varphi^\mu(x_1)$ is the known solution of:

$$\varphi^\mu_{x_1x_1} + \mu^2 f_0(\varphi^\mu) = 0, \quad \varphi^\mu(-\infty) = 0, \quad \varphi^\mu(+\infty) = 1, \ \varphi^\mu(0) = \tfrac{1}{2}. \tag{3.3}$$

Moreover, $\varphi^\mu_{x_1} > 0$, $\varphi^\mu(x_1) = \varphi_1(\mu x_1)$, $\varphi_1(x_1)$ being the solution to (3.3) with $\mu = 1$, and $\varphi^\mu_{x_1}(-x_1) = \varphi^\mu_{x_1}(x_1)$. Substituting v for u in (3.1) gives

$$\nabla_x(1+\delta\lambda a_1)(\nabla_x\varphi^\mu+\delta\nabla_x v)+\delta\lambda b_1(\nabla_x\varphi^\mu+\delta\nabla_x v)+\mu^2 f(\varphi^\mu+\delta v)=0, \tag{3.4}$$

or

$$(\varphi^\mu_{x_1x_1}+\delta\,\triangle_x\, v)+\delta\lambda\nabla_x(a_1(\nabla_x\varphi^\mu+\delta\nabla_x v))+\delta\lambda b_1(x)\cdot\nabla_x\varphi^\mu$$
$$+\delta^2\lambda b_1(x)\cdot\nabla_x v+\mu^2 f(\varphi^\mu+\delta v)=0,$$

or by (3.3):

$$\delta\,\triangle_x\, v+\delta\lambda\nabla_x(a_1(\nabla_x\varphi^\mu+\delta\nabla_x v))+\delta\lambda b_1(x)\cdot\nabla_x\varphi^\mu$$
$$+\delta^2\lambda b_1(x)\cdot\nabla_x v+\mu^2(f(\varphi^\mu+\delta v)-f_0(\varphi^\mu))=0.$$

Cancelling δ to get

$$\triangle_x v+\lambda\nabla_x(a_1(\nabla_x\varphi^\mu+\delta\nabla_x v))+\lambda b_1(x)\cdot\nabla_x\varphi^\mu+\delta\lambda b_1\cdot\nabla_x v+\mu^2\delta^{-1}(f(\varphi^\mu+\delta v)-f_0(\varphi^\mu))=0. \tag{3.5}$$

Eq. (3.5) can be written as:

$$\triangle_x v+\mu^2 f_0'(\varphi^\mu)v\equiv R=R(v)=-\lambda\nabla_x(a_1\nabla_x\varphi^\mu)-\lambda\delta\nabla_x(a_1\nabla_x v)-\lambda b_1\cdot\nabla_x\varphi^\mu-\delta\lambda b_1\cdot\nabla_x v$$
$$-\tfrac{1}{2}\mu^2\delta v^2 f_0''(\varphi^\mu)+\mu^2\delta^2 v^3-\mu^2(1-\varphi^\mu-\delta v)(\varphi^\mu+\delta v). \tag{3.6}$$

The linear operator (on $L^2(\mathbb{R}^1\times T^{n-1})$) on the left hand side of (3.6) has a one dimensional kernel spanned by $\varphi^\mu_{x_1}$, and zero is a simple eigenvalue due to v being periodic in y. Regarding (3.6) as a linear equation for v with v in $R(v)$ given, then to solve (3.6) R must satisfy the following solvability condition:

$$\int\limits_{\mathbb{R}^1\times T^{n-1}} R(v)\varphi^\mu_{x_1}dx_1dy=0. \tag{3.7}$$

We choose λ so that (3.7) holds for any given v such that $R(v)\in L^2(\mathbb{R}^1\times T^{n-1})$. This is possible for δ small and v bounded in $H^2(\mathbb{R}^1\times T^{n-1})$ if

$$\int\limits_{\mathbb{R}^1\times T^{n-1}} \varphi^\mu_{x_1}(\nabla_x(a_1\nabla_x\varphi^\mu)+b_1\cdot\nabla_x\varphi^\mu)dx_1dy\neq 0, \tag{3.8}$$

whose left hand side is equal to:

$$\int\limits_{\mathbb{R}^1}dx_1\int\limits_{T^{n-1}}dy\varphi^\mu_{x_1}[(a_1^{11}\varphi^\mu_{x_1})_{x_1}+(a_1^{21}\varphi^\mu_{x_1})_{x_2}+\cdots+(a_1^{n1}\varphi^\mu_{x_1})_{x_n}]+\int\limits_{\mathbb{R}^1}dx_1\int\limits_{T^{n-1}}dyb_{1,1}(x)(\varphi^\mu_{x_1})^2$$
$$=\int\limits_{\mathbb{R}^1}dx_1\int\limits_{T^{n-1}}dy(\varphi^\mu_{x_1}(a_1^{1,1}\varphi^\mu_{x_1})_{x_1}+b_{1,1}(x)(\varphi^\mu_{x_1})^2)$$
$$=\int\limits_{\mathbb{R}^1}dx_1\int\limits_{T^{n-1}}dy(\tfrac{1}{2}a^{1,1}_{1,x_1}(\varphi^\mu_{x_1})^2+b_{1,1}(x)(\varphi^\mu_{x_1})^2).$$

So we have

$$\int\limits_{\mathbb{R}^1}(\tfrac{1}{2}\langle a^{1,1}_{1,x_1}\rangle_y+\langle b_{1,1}(x)\rangle_y)(\varphi^\mu_{x_1})^2dx_1\neq 0. \tag{3.9}$$

It is easy to see that if condition (3.9) holds, then Eq. (3.6) admits a smooth solution $v \in L^2(\mathbb{R}^1 \times T^{n-1})$ if $\delta = \delta(\mu)$ is small enough, and $\lambda = \lambda(\delta, \mu)$. This is achieved by a standard iteration scheme in a Sobolev space $H^s(\mathbb{R}^1 \times T^{n-1})$, with s large enough, and the contraction mapping principle. In other words, if (3.9) holds, then there is a stationary solution to Eq. (3.1) along direction x_1 taking zero and one at x_1 infinities. By Theorem 2.3, we see that traveling waves do not exist, and there is no front propagation. Thus (3.9) is a sufficient condition for quenching.

The first term inside the integral of (3.9) is the averaged form of the integrand appearing in the one space dimensional quenching condition, see Xin [35]. The conditions for waves going along other directions can be derived similarly. Let us consider some examples.

Example 1: Suppose that $n = 2$, $a^{1,1}(x,y) = 1 + \delta\lambda \sin x (\sin y)^2$, $a^{1,2}(x,y) = a^{2,1}(x,y) = 0$, $a^{2,2}(x,y) = a^{1,1}(x,y)$, and $b(x,y) = (0,0)$, and $f(u) = \mu^2 u(1-u)(u - \frac{1}{2} + \delta)$. Namely, we have the equation:

$$u_t = (a^{1,1}(x,y)u_x)_x + (a^{1,1}(x,y)u_y)_y + f(u). \tag{3.10}$$

Condition (3.9) reduces to:

$$\int_{\mathbb{R}^1} \cos x (\varphi_x^\mu)^2 dx \neq 0, \tag{3.11}$$

which is just the quenching condition in one space dimensional case, and there exists $\mu > 0$, such that (3.11) is satisfied, see Xin [35]. So quenching occurs in x direction. Similarly, if $a^{1,1}(x,y) = 1 + \delta\lambda(\sin x + \sin y)$, and the rest data remain the same, condition (3.9) also holds and quenching occurs in x direction.

Example 2: Suppose that $n = 2$, $a^{1,1}(x,y) = 1 + \delta\lambda \sin x \sin y$, and the rest are the same as in Example 1. Then condition (3.9) is never satisfied, and quenching may or may not occur. For instance, it may occur when δ is not small, and so the standing waves are not captured by the perturbation method.

Example 3: Suppose that $a(x)$= identity matrix, $x = (x_1, y)$, $y \in T^{n-1}$, and $b(x)$ is any divergence free mean zero vector field. Then condition (3.9) reads

$$\int_{\mathbb{R}^1} \langle b(x) \rangle_y (\varphi_{x_1}^\mu)^2 dx_1 \neq 0. \tag{3.12}$$

However, averaging div $b = 0$ over $y \in T^{n-1}$, we see that $(d/dx_1)\langle b(x) \rangle_y = 0$, and thus $\langle b(x) \rangle_y$ = constant = 0. Condition (3.9) fails. It is straightforward to check that (3.9) also fails in any other direction. In fact, it is possible that there is no quenching in the shear flow case. As for other incompressible flows more complicated than shear flows, we describe our numerical studies in the coming sections.

Example 4: If we allow $b(x)$ in example 3 to be compressible yet still having zero mean over T^n, then condition (3.9) is easily satisfied. Take $n = 2$, and $b(x) = (\cos x (\sin y)^2, 0)$, then there is quenching in x_1 direction.

4. Numerical method

In this section, we present a second-order finite difference method to solve Eq. (1.1) numerically in the two-dimensional case. Let us reorder and modify Eq. (1.1) to the following form:

$$u_t + v \cdot \nabla u = \epsilon \nabla \cdot (a(x,y)\nabla u) + \frac{1}{\epsilon} f(u), \tag{4.1}$$

with initial condition

$$u|_{t=0} = u_0(x,y), \tag{4.2}$$

and boundary conditions

$$u|_{x\to-\infty} = 0, \quad u|_{x\to\infty} = 1, \quad u|_{y=1} = u|_{y=0}. \tag{4.3}$$

Here $u(x,y,t)$ is a scalar function representing either the temperature of the combustible gas or the mass fraction of certain reacting species. We have changed the notation for convection from $b(x,y)$ to $-\boldsymbol{v}(x,y)$ to emphasize the physical velocity field. Here it is a given incompressible velocity field, periodic in both x and y directions, and satisfies

$$\langle \boldsymbol{v}(x,y)\rangle_x = \langle \boldsymbol{v}(x,y)\rangle_y = 0, \tag{4.4}$$

where $\langle\ \rangle_x$ and $\langle\ \rangle_y$ represent averaging in x and y directions, respectively. Also in Eq. (4.1) $a(x,y)$ is the given diffusion coefficient, $f(u)$ is the bistable reaction function, and ϵ is a positive suitably small parameter. The parameter ϵ is used to adjust the widths of the fronts so that their spreading is inside our computational domain throughout the time period that we are interested. On the other hand, the size of ϵ is chosen not to be too small to render the resolution of our finite difference scheme difficult. We are studying those particular wave fronts that presumably propagate from the right to the left. The initial profile is usually like a one dimensional planar front along the x direction and independent of y.

The second-order scheme we use to approximate Eq. (4.1) is based on a Crank–Nicholson type scheme where the linear convection is explicitly handled by a second-order upwind approach and the reaction nonlinearity is implicitly solved. For discretization, we partition the computational domain into a collection of rectangular cells, with cell centers $\boldsymbol{x}_{i,j} = \left((i-\frac{1}{2})\Delta x, (j-\frac{1}{2})\Delta y\right)$, and Δx and Δy being the cell sizes. The finite difference solution $u^n_{i,j}$ is defined to approximate u at the centers of cells (i,j) at $t = n\Delta t$, with Δt being the time step. For the velocity field, the x-component v_1 is defined on the vertical cell edges $(i+\frac{1}{2}, j)$, and the y-component v_2 is defined on the horizontal cell edges $(i, j+\frac{1}{2})$. We use this so-called staggered grid for the velocity field because of the simplicity it provides when used to represent an incompressible velocity field in discretized form. With these definitions, the Crank–Nicholson discretization of the equation can be written as the following nonlinear system:

$$\frac{u^{n+1}_{i,j} - u^n_{i,j}}{\Delta t} + (\boldsymbol{v}\cdot\nabla u)^{n+1/2}_{i,j} = \left(L_h(a)\frac{u^n + u^{n+1}}{2}\right)_{i,j} + \frac{f(u^n_{i,j}) + f(u^{n+1}_{i,j})}{2}, \tag{4.5}$$

with the velocity $\boldsymbol{v} = (v_1, v_2)$ satisfying the discrete divergence-free condition:

$$(D\boldsymbol{v})_{i,j} = \frac{v_{1,i+1/2,j} - v_{1,i-1/2,j}}{\Delta x} + \frac{v_{2,i,j+1/2} - v_{2,i,j-1/2}}{\Delta y} = 0. \tag{4.6}$$

The discrete diffusion operator $L_h(a)$ is an approximation to the variable diffusion term. If we write $a_{i+1/2,j+1/2} = a(x_{i+1/2}, y_{j+1/2})$, the second-order approximation is:

$$\begin{aligned}(L_h(a)u)_{i,j} = {} & \frac{a_{i+1/2,j}u_{i+1,j} + a_{i-1/2,j}u_{i-1,j} - (a_{i+1/2,j} + a_{i-1/2,j})u_{i,j}}{\Delta x^2} \\ & + \frac{a_{i,j+1/2}u_{i,j+1} + a_{i,j-1/2}u_{i,j-1} - (a_{i,j+1/2} + a_{i,j-1/2})u_{i,j}}{\Delta y^2}.\end{aligned} \tag{4.7}$$

It remains to describe the approximation of the linear convection term $(v \cdot \nabla u)^{n+1/2}$, which is treated explicitly as a forcing term of the Crank–Nicholson system. Here we choose a second-order conservative approximation

$$(v \cdot \nabla u)_{i,j}^{n+1/2} = \frac{v_{1,i+1/2,j} u_{i+1/2,j}^{n+1/2} - v_{1,i-1/2,j} u_{i-1/2,j}^{n+1/2}}{\Delta x} + \frac{v_{2,i,j+1/2} u_{i,j+1/2}^{n+1/2} - v_{2,i,j-1/2} u_{i,j-1/2}^{n+1/2}}{\Delta y}, \tag{4.8}$$

by assuming the edge values of u, whereas the edge velocities are naturally given by our choice of the staggered grid for the discrete velocity field. The edge values of u at the half time steps are calculated from an upwind method based on ideas introduced by Colella [14] which requires no splitting to handle the two-dimensional effects. This method is second-order accurate for smooth solutions and stable in regions with steep gradients. For example, to calculate the edge values $u_{i+1/2,j}^{n+1/2}$ along the vertical edges, we extrapolate from both the left and the right cells using Taylor series expansions in both space and time,

$$\begin{aligned} u_{i+1/2,j}^{L} &= u_{i,j}^{n} + \tfrac{1}{2}\Delta x u_{x,i,j} + \tfrac{1}{2}\Delta t u_{t,i,j}, \\ u_{i+1/2,j}^{R} &= u_{i+1,j}^{n} - \tfrac{1}{2}\Delta x u_{x,i+1,j} + \tfrac{1}{2}\Delta t u_{t,i+1,j}. \end{aligned} \tag{4.9}$$

The time derivative can be eliminated by using Eq. (4.1) and the resulting extrapolations are:

$$\begin{aligned} u_{i+1/2,j}^{L} &= u_{i,j}^{n} + \tfrac{1}{2}\Delta x(1 - v_{1,i,j}\frac{\Delta t}{\Delta x}) u_{x,i,j} - \tfrac{1}{2} v_{2,i,j}\Delta t u_{y,i,j} + \tfrac{1}{2}\Delta t \left[\epsilon (L_h(a)u^n)_{i,j} + \frac{1}{\epsilon} f(u_{i,j}^n)\right], \\ u_{i+1/2,j}^{R} &= u_{i+1,j}^{n} - \tfrac{1}{2}\Delta x(1 + v_{1,i+1,j}\frac{\Delta t}{\Delta x}) u_{x,i+1,j} - \tfrac{1}{2} v_{2,i+1,j}\Delta t u_{y,i+1,j} + \tfrac{1}{2}\Delta t \left[\epsilon (L_h(a)u^n)_{i+1,j} + \frac{1}{\epsilon} f(u_{i+1,j}^n)\right]. \end{aligned} \tag{4.10}$$

Here the velocity $(v_{1,i,j}, v_{2,i,j})$ is taken to be the average of the edge velocities

$$v_{1,i,j} = \tfrac{1}{2}(v_{1,i+1/2,j} + v_{1,i-1/2,j}), \quad v_{2,i,j} = \tfrac{1}{2}(v_{2,i,j+1/2} + v_{2,i,j-1/2}). \tag{4.11}$$

We are now left with the approximations to the space derivatives $u_{x,i,j}$ and $u_{y,i,j}$. For approximations to vertical edges, u_x is considered to be along the normal direction and u_y is considered to be along the transverse direction. These two space derivatives should be approximated differently, according to [14], for stability considerations. Namely, the normal derivative u_x is approximated by the central difference with the Van Leer limiter:

$$u_{x,i,j} = \begin{cases} \dfrac{1}{\Delta x}\operatorname{sign}(\Delta u)\min\left(2|\Delta u_L|, 2|\Delta u_R|, |\Delta u|\right), & \Delta u_L \cdot \Delta u_R > 0, \\ 0, & \Delta u_L \cdot \Delta u_R \le 0, \end{cases} \tag{4.12}$$

where

$$\Delta u = \tfrac{1}{2}(u_{i+1,j} - u_{i-1,j}), \quad \Delta u_L = u_{i,j} - u_{i-1,j}, \quad \Delta u_R = u_{i+1,j} - u_{i,j}, \tag{4.13}$$

and the transverse derivative u_y is approximated by a first-order upwind difference:

$$u_{y,i,j} = \begin{cases} \dfrac{u_{i,j} - u_{i,j-1}}{\Delta y}, & v_{2,i,j} \ge 0, \\ \dfrac{u_{i,j+1} - u_{i,j}}{\Delta y}, & v_{2,i,j} < 0. \end{cases} \tag{4.14}$$

The idea behind this is that we want the second-order scheme to be reduced to the first-order corner-transport-upwind (CTU) scheme when the gradient of the solution becomes steep, where the CTU scheme is still stable.

For details of this we refer to [14]. Once we have the space derivative approximations, we can calculate $u^L_{i+1/2,j}$ or $u^R_{i+1/2,j}$ accordingly and the correct value is taken from the side according to the sign of the edge velocity,

$$u^{n+1/2}_{i+1/2,j} = \begin{cases} u^L_{i+1/2,j}, & v_{1,i+1/2,j} \geq 0, \\ u^R_{i+1/2,j} & v_{1,i+1/2,j} < 0. \end{cases} \tag{4.15}$$

The same technique is used for the approximations of horizontal edge values.

This part of the scheme to calculate the flow flux is explicit and therefore requires the time step Δt to satisfy the Courant–Friederchs–Lewy condition

$$\Delta t \leq \min\left(\frac{h}{|v_{1,i+1/2,j}|}, \frac{h}{|v_{2,i,j+1/2}|}\right). \tag{4.16}$$

Now we can write the nonlinear system in the following form:

$$u^{n+1}_{i,j} - \tfrac{1}{2}\Delta t\left[(L_h(a)u^{n+1})_{i,j} + f(u^{n+1}_{i,j})\right] = F(u^n)_{i,j}, \tag{4.17}$$

with the given forcing term

$$F(u^n)_{i,j} = u^n_{i,j} + \tfrac{1}{2}\Delta t\left[(L_h(a)u^n)_{i,j} + f(u^n_{i,j})\right] - \Delta t(v\cdot\nabla u)^{n+1/2}_{i,j}. \tag{4.18}$$

The boundary conditions are prescribed in the following way: we choose a finite domain $[-x_L, x_L] \times [0,1]$ with the condition that the length of the numerical domain x_L is large enough to cover the wave in the time period that we are interested. Therefore, we can impose

$$u|_{x=-x_L} = 0, \quad u|_{x=x_L} = 1, \quad u|_{y=1} = u|_{y=0}. \tag{4.19}$$

To solve this nonlinear system, we use a nonlinear package NKSOL ([11,16]), which uses a GMRES iterative scheme. We found it very effective in this study.

Next we describe briefly the velocity field used here. For this study, we choose a simple steady velocity field satisfying the discrete divergence-free condition (4.6). As later works proceed, we will consider more complicated flow fields and the coupling of the convection velocity and the reacting variables. To study the effect of convection, we require that this velocity field have zero mean flux in either of the two directions. The flow generated by a periodic array of vortices serves as a good candidate for this purpose, but it does not necessarily satisfy the discrete divergence-free condition. We then modify the velocity field to satisfy Eq. (4.6). To do this, we take a projection step and use the discretely divergence-free part in our calculations. The streamline contour plot of the field is shown in Fig. 1. The solid curves are for counter-clockwise rotating flow fields and the dotted curves are for clockwise rotating flow fields. The details of this velocity field can be found in [38]. There is a vortex length scale λ in this construction and here we choose $\lambda^2 = 0.15$.

5. Numerical results

To make our results comparable to those in [35], we choose $\epsilon = 0.05$ in Eq. (4.1); and the domain for calculations is $[-x_L, x_L] \times [0,1]$ with $x_L = 1$ or 2, depending on the coverage needed for the wave. The case $x_L = 1$ is equivalent to the numerical domain in [35] with a constant scaling factor of 5, both in time and space. The strength of the velocity field is measured by its root-mean-square value. For the diffusive media coefficient, we consider the following three forms:

$$a^{1,1}(x,y) = a_1(x,y) = 1 + \delta\sin(\omega x), \tag{5.1}$$

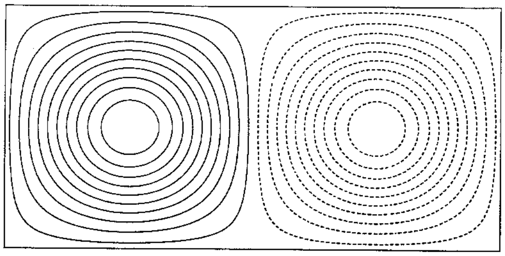

Fig. 1. Streamline contour of the velocity field.

or

$$a^{1,1}(x,y) = a_2(x,y) = 1 + \tfrac{1}{2}\delta(\sin(\omega x) + \sin(\omega y)), \tag{5.2}$$

or

$$a^{1,1}(x,y) = a_3(x,y) = 1 + \delta \sin(\omega x)\sin(\omega y), \tag{5.3}$$

with $\omega = 100$ chosen to be consistent with the choice in [35]. In either of the above choices, we set $a^{1,2} = a^{2,1} = 0$, and $a^{2,2} = a^{1,1}$. The parameter δ in (5.1), (5.2), and (5.3) differs from the δ in Section 3 by a factor λ, and the δ here does not have to be very small.

Throughout our calculations, we start with the following initial condition, which is like a wave profile in the x-direction:

$$u|_{t=0} = \begin{cases} 0, & x \le x_f - 0.1, \\ 5(x - x_f + 0.1), & x_f - 0.1 < x \le x_f + 0.1, \\ 1, & x > x_f + 0.1, \end{cases} \tag{5.4}$$

where x_f is a parameter to locate the initial front. Unless otherwise noted, we choose $x_f = 0.7$ to locate the initial fronts in our calculations. We use uniform grids, $\Delta x = \Delta y = 1/128$, with sizes either 256×128 or 512×128, corresponding to $x_L = 1$ or $x_L = 2$, respectively. We have results from a more refined grid for certain cases and the pictures do not differ substantially. For computational convenience we will use the grid $h = \Delta x = \Delta y = 1/128$ throughout the calculations given below. For all the surface plots with $x_L = 2$, only a section of the domain with length 2 which contains the dynamics of the wave front is shown. The omitted parts are constant states with either $u = 0$ or $u = 1$.

Let us consider $a^{1,1} = a_1$ as in (5.1). First, we choose $\mu = 0.365$, $\delta = 0.96$, which correspond to the starting values in [35], and study the effect of the convection on the propagation. The case $rms = 0$ is reduced to the one-dimensional case studied in [35] and we verified that our solutions agree with that in [35]. In Fig. 2 the one-dimensional profiles at $t = 2, 4, 6$ and 8 are plotted. Notice that the wave is propagated from the left to the right with a steady speed. Then we add the convection term and increase the rms value gradually to study the effects of the flow field. In the left column of Fig. 3, we show the surface plot of u at $t = 2, 4$ and 8 with $rms = 0.125$, which is a rather weak flow field, and we observe that the wave is accelerated with the presence of the velocity field. Next we increase the rms value to 0.25 and the results are plotted in the right column of Fig. 3. In comparison of these two cases, we notice that the wave structures are similar, but the larger rms value produces a more enhanced propagation. This is only true for small values of rms, results for large rms will show otherwise, as we will discuss later.

In [35] it was found that, without the convection, at $\mu = 0.365$ quenching is observed by increasing δ from 0.96 to 0.98. One would expect from the above discussion of the effect of weak flow fields that quenching may

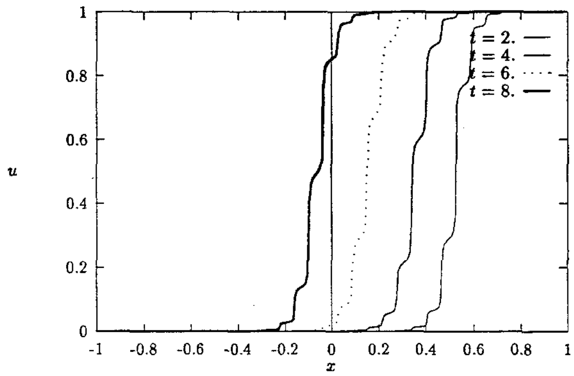

Fig. 2. One-dimensional solutions at $t = 2, 4, 6$ and 8.

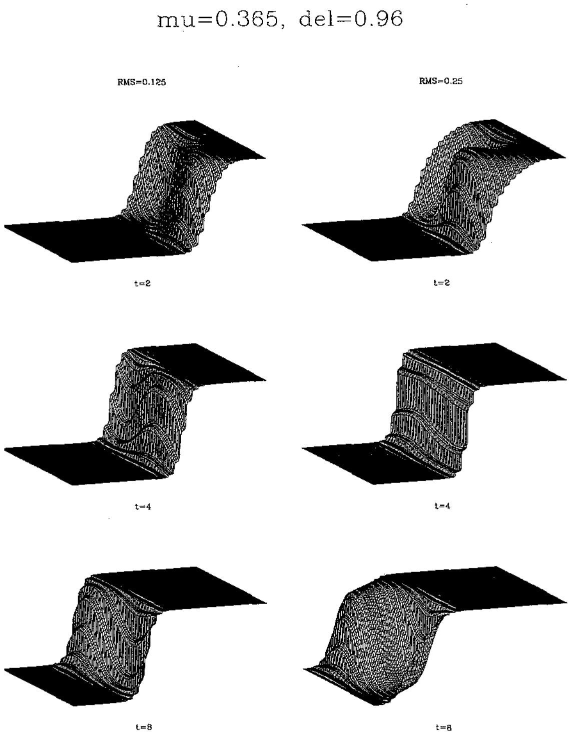

Fig. 3.

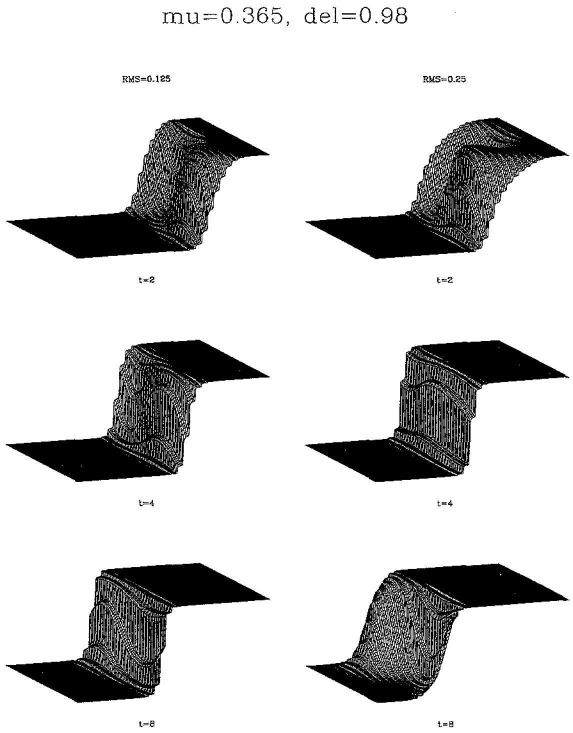

Fig. 4.

Fig. 3. Propagating fronts for $\mu = 0.365, \delta = 0.96$ and $rms = 0.125$, 0.25.

Fig. 4. Propagating fronts for $\mu = 0.365, \delta = 0.98$ and $rms = 0.125$, 0.25.

no longer exist for this δ value if we add in the convection by a small amount. In Fig. 4 we indeed find this to be the case, where we set the *rms* value to 0.125 and 0.25. Quenching is not observed and the propagation is enhanced by the larger *rms* value, as long as the value is still small compared to 1. Another factor in the quenching phenomenon is the value of μ. A larger value of μ is certainly to slow down the propagation of the front. The question is at what value of μ quenching starts to happen with δ fixed. In the one-dimensional case quenching is observed at $\mu = 0.43$ with $\delta = 0.96$. For the same μ, in the two-dimensional case involving

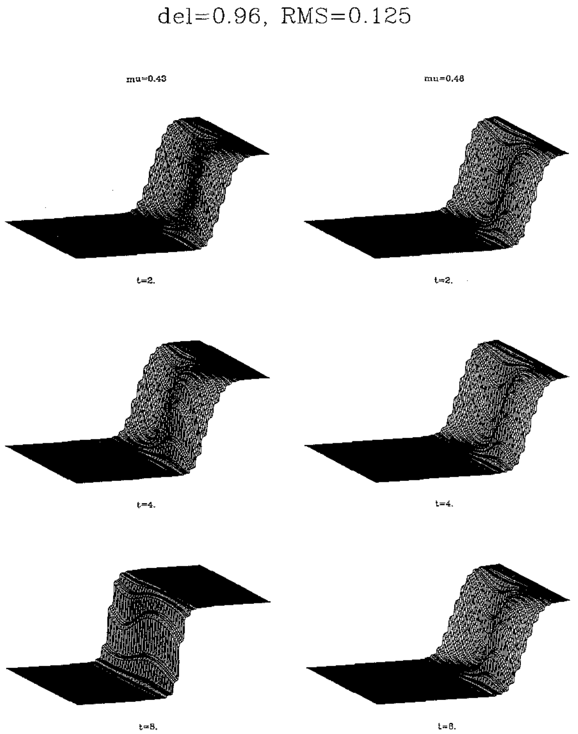

Fig. 5.

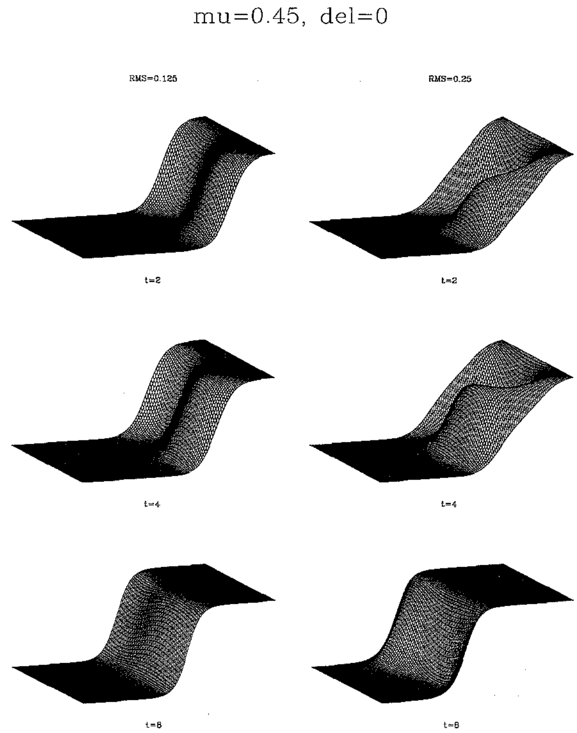

Fig. 6.

Fig. 5. Propagating fronts for $\delta = 0.96, rms = 0.125$, with two cases $\mu = 0.43$ and $\mu = 0.48$.

Fig. 6. Propagating fronts for $\mu = 0.45, \delta = 0$, with two cases $rms = 0.125$ and $rms = 0.25$.

a weak flow field ($rms = 0.125$), the propagation is enhanced. We find quenching only at $\mu = 0.48$, as plotted in Fig. 5. In column 1 of Fig. 5 where $\mu = 0.43$, the wave is still propagating to the left at $t = 8$, but column 2 ($\mu = 0.48$) clearly shows the approaching of a steady state.

One extreme case we are particularly interested in is when $\delta = 0$, where the diffusive media is uniform and we can eliminate the factor of inhomogeneous diffusion. In Fig. 6 we set $\mu = 0.45$, $\delta = 0$, and so $a = 1$. Again we find that a relatively larger *rms* value (0.25) results in a faster propagation than a relatively smaller *rms* value (0.125). From the above calculations we conclude that weak flow fields enhance wave propagation in the two-dimensional case.

The question is how far one can sustain this enhancing effect by increasing the *rms* value. In turbulent combustion, there is a very important quenching phenomenon caused by excessive flow disturbances which is characterized by large *rms* values. Here we use the relatively simple steady flow field in the hope of gaining some insight into this issue of great practical significance. We study the cases with or without diffusion disturbances. The case without diffusion disturbances ($\delta = 0$) is particularly interesting. It is known in the one-dimensional case that travelling waves exist for any $0 < \mu < 0.5$ if there is no disturbances in diffusion, therefore we can attribute the quenching phenomenon directly to the flow field disturbance if it is observed. In Fig. 7, we plot the results for the case $\mu = 0.45, \delta = 0$, and $rms = 1$ at $t = 0.25, 0.5, 1, 2, 4$, and 8. This flow is so much stronger than the previous ones that the front is being wrapped by the flow at $t = 0.25$, then it retreats due to the reaction term with the large μ value at $t = 1$. At $t = 2$ the front starts to reach its steady state, as we see in the subsequent plots. As we know, a wavy front without convection will be flattened by the bistable

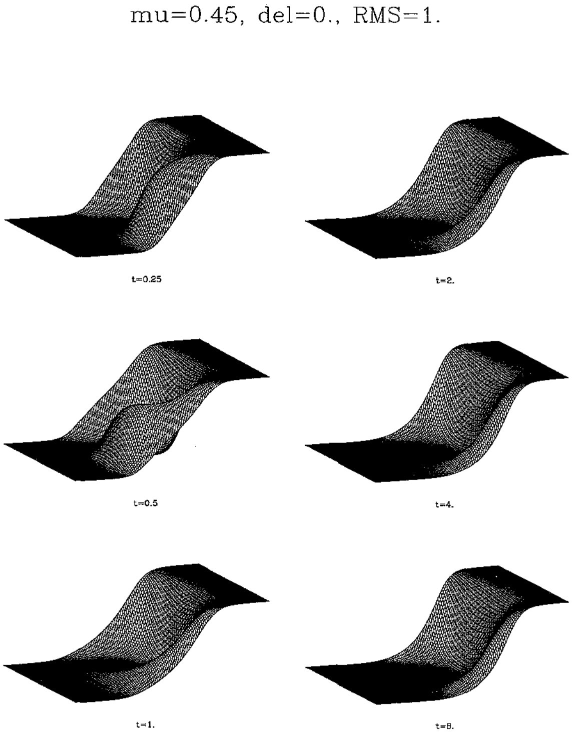

Fig. 7.

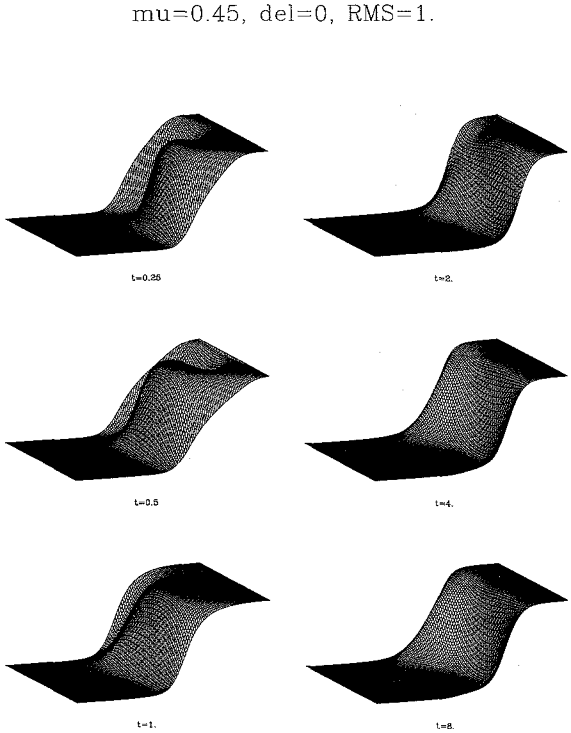

Fig. 8.

Fig. 7. Propagating fronts for $\mu = 0.45, \delta = 0, rms = 1$, with $x_f = 0.7$.

Fig. 8. Propagating fronts for $\mu = 0.45, \delta = 0, rms = 1$, with $x_f = 0.3$.

reaction and the convection itself tends to wrinkle the front. This example suggests an equilibrium between the flow field and the reaction, and indicates that quenching due to excessive flow field does occur in the bistable reaction, even without the diffusive inhomogeneities.

We note that if $u_S(x, y)$ is a steady state solution to Eq. (4.1), taking zero and one at x infinities, then $u_S(x + np, y)$, where p is the period of the media, and n is any integer, is also such a steady state solution. Thus such steady states form at least a one-parameter family. If there is quenching, the initial transient fronts will run into one of the steady states of this family or other. The fronts should presumably settle down to the ones that are most attracting. Imagine that these steady states were walls standing in front of the waves. If the first wall a wave hits is more attracting than its neighbors, then the wave will just attach to this wall and approach steady state there. But if it is not as attracting as one of its neighbors, the wave is first reflected, then retreats, and finally ends up attaching to the next wall. This may explain the different front behaviors we see above before quenching is realized. To verify this point, we change the initial front location from $x_f = 0.7$ to $x_f = 0.3$ and repeat the calculation in Fig. 7. The results are shown in Fig. 8 and we observe that the steady state here is exactly the reflection image of that in Fig. 7, which indicates that this initial transient front has run into a neighboring steady state of the family. It is expected to see alternating reflection images for the steady states in the family since our velocity field has a counter-rotating periodic feature in that direction. We want to point out that for this case it takes longer to settle to the steady state. As we see from Fig. 8, for $t \leq 1$ the flow is wrapping the front in the clockwise direction, just in the same way as in Fig. 7, but then the reaction tries to flatten the front and leads the front to the next cell with a counter-clockwise rotation field. Eventually

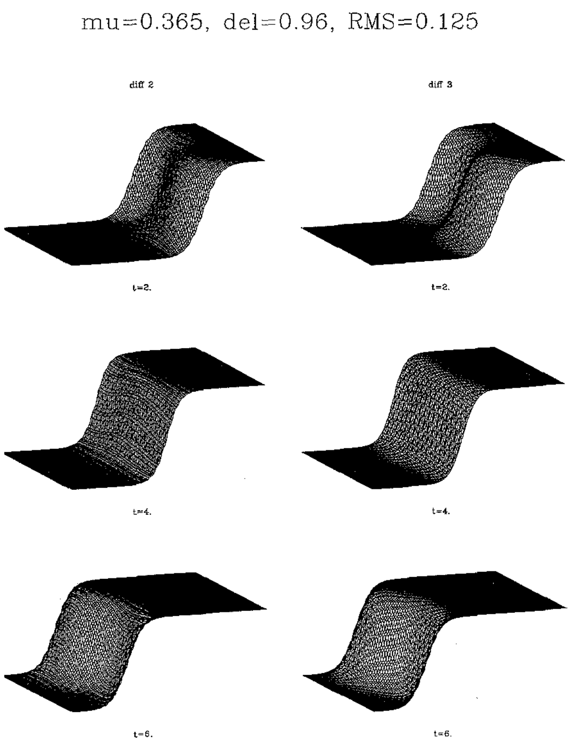

Fig. 9.

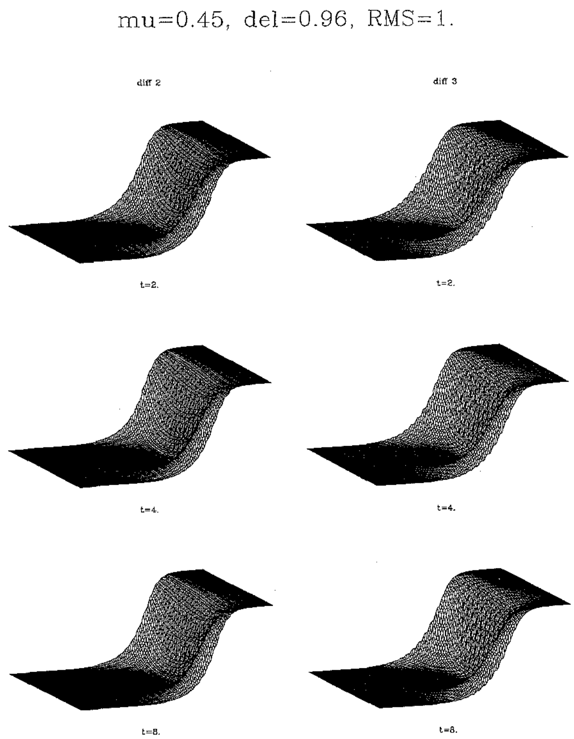

Fig. 10.

Fig. 9. Propagating fronts for $\mu = 0.365, \delta = 0.96, rms = 0.125$ with diffusion coefficients a_2 and a_3.

Fig. 10. Propagating fronts for $\mu = 0.45, \delta = 0.96, rms = 1$ with diffusion coefficients a_2 and a_3.

the front is wrapped by the counter-clockwise rotation and reaches the next steady state in the family. Also we notice that by $t = 2$ the front has not reached the steady state yet, in comparison with the same time picture in Fig. 7. This just shows that the wave in this case is not as close to the attractor as in the previous case.

In all the above calculations we have assumed that the diffusion coefficient has the form a_1 (Eq. (5.1)). In Fig. 9, we show the results corresponding to the diffusion coefficients a_2 and a_3 with a relatively small *rms* value. The propagation structures are similar to the case of a_1. In Fig. 10, we increase the *rms* value to 1 trying to observe the quenching phenomenon. Column 1 corresponds to a_2, in this case the sufficient condition for quenching given in Section 3 is satisfied and we have a steady state similar to that in Fig. 7. The case of a_3 is more interesting since the sufficient condition is not satisfied there. But our numerical result (column 2) does show a steady state similar to column 1. A comparison of Fig. 10 with Fig. 7 reveals that the global front structures in all 3 cases (with $rms = 1$ and $\mu = 0.45$ but $a^{1,1} = 1$, in Fig. 7, and $a^{1,1} = a_2$, a_3 with $\delta = 0.96$ in Fig. 10) are very similar, the only difference being the details of local fluctuations. This suggests that the quenching behavior due to flows with large fluctuations is dominated by the flow fields and the diffusive inhomogeneities play a lesser role. It is our hope that this can be established for more general and complex turbulent flows.

6. Conclusion

Using analytical and numerical methods, we have studied the front dynamics of the bistable reaction-diffusion equations with convective-diffusive periodic coefficients in several space dimensions. The convection effect is displayed in a twofold way. In two space dimensions, we observe front quenching if the incompressible convective flow fields have a large enough root mean square value. The diffusive inhomogeneities are subject to the strong convection effects and do not seem to change the quenching phenomenon qualitatively in the strong convection regime. We also observe that weak convection fields enhance the propagation and so may remove quenching caused by diffusive inhomogeneities. We showed a sufficient condition for quenching, and the performed numerical calculations agree with it in cases it applies. We hope to discuss the front dynamics in the systems of bistable reaction-diffusion equations with complex flow fields in the future.

Acknowledgements

J.X. Xin acknowledges the support of National Science Foundation grant DMS-9302830. JYZ would like to thank Dr. Jeff McGough for his help with use of the NKSOL package. We thank Paul Fife for his interest and comments. The calculations were performed at the Utah Supercomputing Institute.

References

[1] D.G. Aronson and H.F. Weinberger, Multidimensional nonlinear diffusion arising in population genetics, Advances in Mathematics 30 (1978) 33–76.
[2] G. Barles, L.C. Evans, P.E. Souganidis, Wavefront propagation for reaction-diffusion systems of PDE, Duke Math. J. 61, No.3 (1990).
[3] A. Bensoussan, J.L. Lions and G. Papanicolaou, Asymptotic Analysis for Periodic Structures, Studies in Mathematics and its Applications, Vol. 5, (North-Holland, Amsterdam, 1978).
[4] H. Berestycki, B. Nicolaenko and B. Scheurer, Travelling wave solutions to combustion models and their singular limits, SIAM J. Math. Anal. 16(6) (1985) 1207–1242.
[5] H. Berestycki, L. Nirenberg, Some Qualitative Properties of Solutions of Semilinear Elliptic Equations in Cylindrical Domains. Analysis etc, eds. P. Rabinowitz et al. (Academic Press, New York, 1990) pp. 115–164.
[6] H. Berestycki, L. Nirenberg, On the method of moving planes and the sliding method, Bol. da. Soc. Brasileira de Mathematica 22 (1991) 1–37.
[7] H. Berestycki, L. Nirenberg, Traveling fronts in cylinders (1992), preprint.
[8] H. Berestycki, B. Larrouturou, A semi-linear elliptic equation in a strip arising in a two-dimensional flame propagation model, J. Reine Angew. Math. 396 (1989) 14–40.
[9] H. Beresticki, B. Larrouturou and P.L. Lions, Multi-dimensional travelling-wave solutions of a flame propagation model, Arch. Rat. Mech. Anal. 111 (1990) 33–49.
[10] H. Berestycki and G. Sivashinsky, Flame extinction by periodic flow field, SIAM J. Appl. Math., Vol. 51, No. 2 (1991) 344–350.
[11] P.N. Brown and Y. Saad, Hybrid Krylov Methods for Nonlinear Systems of Equations, LLNL Report UCRL-97645 (1987).
[12] A. Chorin, Numerical solution of the Navier-Stokes equations, Math. Comp. 22 (1968) 742.
[13] P. Clavin and F.A. Williams, Theory of premixed-flame propagation in large-scale turbulence, J. Fluid Mech. 90 (1979) 598–604.
[14] P. Colella, Multidimensional upwind methods for hyperbolic conservation laws, J. Comp. Phys. 87 (1990) 171.
[15] G. Dagan and S.P. Neuman, Nonasymptotic behavior of a common Eulerian approximation for transport in random velocity fields, Water Resour. Res. 27 (1991) 3249–3256.
[16] J.E. Dennis and R.B. Schnabel, Numerical Methods for Unconstrained Optimization and Nonlinear Equations (Prentice-Hall, Englewood Cliffs, NJ, 1983).
[17] P.C. Fife and J.B. McLeod, The approach of solutions of nonlinear diffusion equations to travelling front solutions, Arch. Rat. Mech. Anal. 65 (1977) 355–361.
[18] M. Freidlin, Functional Integration and Partial Differential Equations, Annals of Mathematics Studies, Vol. 109 (Princeton Univ. Press, Princeton, 1985).
[19] M.I. Freidlin, Geometric optics approach to reaction-diffusion equations, SIAM J. Appl. Math. 46 (1986).

[20] J. Gartner and M.I. Freidlin, On the propagation of concentration waves in periodic and random media, Dokl. Acad. Nauk SSSR 249 (1979) 521–525.
[21] A. Friedman, Partial Differential Equations of Parabolic Type, (Prentice-Hall, Englewood Cliffs, NJ, 1964).
[22] J. Hanna, A. Saul and K. Showalter, Detailed studies of propagating fronts in the iodate oxidation of arsenous acid reaction, J. Phys. Chem. 90 (1986) 225.
[23] A. Kolmogorov, I. Petrovskii and N. Piskunov, A study of the equation of diffusion with increase in the quantity of matter and its application to a biological problem, Bjul. Moskovskogo Gos. Univ. 1:7 (1937) 1–26.
[24] C. Li, Ph.D. Thesis, Courant Inst., NYU (1989).
[25] J. Pauwelussen, Nerve impulse propagation in a branching nerve system: A simple model, Physica D. 4 (1981) 67–88.
[26] G. Papanicolaou, X. Xin, Reaction-diffusion fronts in periodically layered media, J. Stat. Phys., 63 (1991) 915-931.
[27] J-M. Roquejoffre, Eventual monotonicity and convergence to traveling fronts for the solutions of parabolic equations in cylinders (1992), preprint.
[28] J. Sethian, Turbulent combustion in open and closed vessels, J. Com. Phys. 54 (1984) 425–456.
[29] G.I. Sivashinsky, Cascade-renormalization theory of turbulent flame speed, Combust. Sci. and Tech. 62 (1988) 77–96.
[30] S.R.S. Varadhan, On the behavior of the fundamental solutions of the heat equation with variable coefficients, Comm. Pure and Appl. Math. 20 (1967) 431–455.
[31] S. Yates and C. Ensfield, Transport of dissolved substance with second order reaction, Water Resour. Res. Vol. 25 (1990) 1757–1762.
[32] X. Xin, Existence and stability of travelling waves in periodic media governed by a bistable nonlinearity, J. Dyn. Diff. Eqs. 3 (1991) 541–573.
[33] X. Xin, Existence and uniqueness of traveling waves in a reaction-diffusion equation with combustion nonlinearity, Indiana Univ. Math. Journal 40 (1991) 985–1008.
[34] J.X. Xin, Existence of planar flame fronts in convective diffusive periodic media, Arch. for Rational Mech. and Analys. 121 (1992) 205–233.
[35] J.X. Xin, Existence and nonexistence of traveling waves and reaction-diffusion front propagation in periodic media, J. Stat. Phys. (1993) to appear.
[36] V. Yakhot, Propagation velocity of premixed turbulent flames, Comb. Sci. Tech., 60 (1988) 191–214.
[37] J. Zhu and J. Sethian, Projection methods coupled to level set interface techniques, J. Comp. Phys. 102 (1992) 128.
[38] J. Zhu and P. Ronney, Simulation of front propagation at large non-dimensional flow disturbance intensities, Comb. Sci. Tech., in press.